Executioner caspase-3 and caspase-7 are functionally distinct proteases

John G. Walsh, Sean P. Cullen, Clare Sheridan, Alexander U. Lüthi, Christopher Gerner*, and Seamus J. Martin†

Molecular Cell Biology Laboratory, Department of Genetics, The Smurfit Institute, Trinity College, Dublin 2, Ireland

Edited by Doug R. Green, St. Jude Children's Research Hospital, Memphis, TN, and accepted by the Editorial Board July 8, 2008 (received for review August 15, 2007)

Members of the caspase family of cysteine proteases play central roles in coordinating the stereotypical events that occur during apoptosis. Because the major executioner caspases, caspase-3 and caspase-7, exhibit almost indistinguishable activity toward certain synthetic peptide substrates, this has led to the widespread view that these proteases occupy functionally redundant roles within the cell death machinery. However, the distinct phenotypes of mice deficient in either of these caspases, as well as mice deficient in both, is at odds with this view. These distinct phenotypes could be related to differences in the relative expression levels of caspase-3 and caspase-7 *in vivo*, or due to more fundamental differences between these proteases in terms of their ability to cleave natural substrates. Here we show that caspase-3 and caspase-7 exhibit differential activity toward multiple substrate proteins, including Bid, XIAP, gelsolin, caspase-6, and cochaperone p23. Caspase-3 was found to be generally more promiscuous than caspase-7 and appears to be the major executioner caspase during the demolition phase of apoptosis. Our observations provide a molecular basis for the different phenotypes seen in mice lacking either caspase and indicate that these proteases occupy nonredundant roles within the cell death machinery.

apoptosis | caspase substrates | proteolysis

Apoptosis is a mode of programmed cell death that is coordinated by members of the caspase family of cysteine proteases. Caspases are activated in response to diverse cell death stimuli and ultimately dismantle the cell through restricted proteolysis of numerous cellular proteins that latest estimates suggest number over 400 (1, 2). It is now well established that certain caspases (caspase-8, caspase-9, and caspase-10 in humans) play upstream "initiator" roles in apoptosis by coupling cell death stimuli to the downstream "effector" caspases (caspase-3, caspase-6, and caspase-7). The initiator caspases appear to be highly specific proteases that cleave few proteins other than their own precursors and the downstream effector caspases (3, 4). Thus, the bulk of the proteolysis that takes place during apoptosis is carried out by the effector caspases. However, the relative contributions made by the effector caspases to the demolition phase of apoptosis are still largely unknown.

The specificity profiles observed with caspase-3 and caspase-7, using positional scanning peptide libraries, are virtually indistinguishable (5, 6). This has resulted in a widely held view that caspase-3 and caspase-7 are essentially redundant with respect to the repertoire of substrates that these proteases cleave during apoptosis. However, in direct opposition to this view are the distinct phenotypes of mice deficient in these caspases (7–9). Whereas the majority of mice deficient in caspase-3 on the 129 background die *in utero* or within weeks of birth because of many extra cells within the brains of these animals, caspase-7-deficient mice are viable on the same genetic background (7, 9). However, strain-specific effects of mice deficient in either caspase have also been noted. Caspase-3 deficiency, on the B6 background, has little discernable impact on cell numbers, and such mice are viable (8, 10), as are mice deficient in caspase-7 on the same genetic background (9). However, mice doubly deficient for *CASP-3* and *CASP-7* on the B6 background die immediately after birth because of defective heart development (9). The latter result suggests that there may be a degree of functional compensation in operation between caspase-3 and caspase-7, whereas the knockout phenotypes observed on the 129 background suggest that caspase-3 and caspase-7 serve distinct roles. However, a major problem in interpreting these data is that the relative expression levels of caspase-3 and caspase-7 may vary dramatically between mouse strains, as well as within particular tissues. Indeed, higher intrinsic levels of caspase-7 in B6 mice have been suggested to ameliorate the *CASP-3* knockout phenotype on this background (8). Therefore, it remains unclear whether caspase-3 and caspase-7 are functionally redundant proteases, capable of targeting the same cohort of substrates to coordinate the terminal events in apoptosis.

Using human Jurkat cell-free extracts immunodepleted of either caspase-3 or caspase-7, we have previously shown that removal of caspase-3 abolished cytochrome *c*/dATP-induced proteolysis of numerous caspase substrates in this experimental system (11). By comparison, depletion of caspase-7 from the same cell-free extracts had little effect on the same panel of caspase substrates (11). One interpretation of these data is that caspase-3 is the major effector caspase and is sufficient for proteolysis of the majority of substrates that are cleaved during the terminal phase of apoptosis. However, an alternative interpretation is that caspase-3 is simply a more abundant caspase in certain cell types, such as Jurkat cells. Thus, caspase-7 may be capable of functionally substituting for caspase-3 in situations where both proteases are expressed at similar levels.

To address these issues, we have used purified recombinant caspase-3 and caspase-7 to explore whether these proteases are capable of cleaving the same substrates with similar efficiency. Here we show that although caspase-3 and caspase-7 do appear to be capable of cleaving certain substrates such as PARP, RhoGDI, and ROCK I with a similar efficiency, these proteases exhibit major differences in terms of their ability to cleave many other substrates. Of note, caspase-3 was active toward a much broader array of substrates than caspase-7. These data argue that caspase-3 and caspase-7 are functionally distinct proteases and that caspase-3 is the principal apoptosis-associated effector caspase.

Results and Discussion

Caspase-3 and Caspase-7 Exhibit Differential Activity Toward Synthetic Substrates. Caspase-3 and caspase-7 are both activated universally during apoptosis, irrespective of the specific death-

Author contributions: S.J.M. designed research; J.G.W., S.P.C., C.S., A.U.L., and C.G. performed research; J.G.W., S.P.C., C.G., and S.J.M. analyzed data; and S.J.M. wrote the paper.

The authors declare no conflict of interest.

This article is a PNAS Direct Submission. D.R.G. is a guest editor invited by the Editorial Board.

*Present address: Institute of Cancer Research, Department of Medicine I, Medical University of Vienna, Borschkegasse 8A, 1090 Vienna, Austria.

†To whom correspondence should be addressed. E-mail: martinsj@tcd.ie.

This article contains supporting information online at www.pnas.org/cgi/content/full/0707715105/DCSupplemental.

initiating stimulus, and both proteases are widely considered to coordinate the demolition phase of apoptosis by cleaving a diverse array of protein substrates (1, 2). However, the relative contribution made by these proteases to cellular demolition remains largely speculative. Caspase-3 and caspase-7 are most closely related to each other, as compared with other mammalian caspases, but nonetheless display substantial sequence divergence, with an overall sequence identity of 56% and sequence similarity of 73% (Fig. 1*A*). To explore the substrate preferences of these caspases in more detail, we expressed both enzymes as His-tagged proteins in bacteria and purified these to homogeneity (Fig. 1*B*). Both caspases were active-site-titrated against DEVD-AFC in combination with the polycaspase inhibitor zVAD-fmk (Fig. 1*C*). Based on active-site titration data, the active concentration of each enzyme was normalized to allow for direct comparisons between these enzymes in subsequent experiments (Fig. 1*D*). We then compared these caspases in terms of their ability to hydrolyze a panel of synthetic tetrapeptide substrates. As Fig. 1*E* illustrates, both caspases preferentially cleaved DEVD-AFC with essentially identical efficiency. In contrast, caspase-3 cleaved LEHD-AFC more efficiently than caspase-7, suggesting that these proteases possess distinct activities toward certain synthetic substrates (Fig. 1*E*).

Caspase-3 and Caspase-7 Exhibit Differential Activity Toward Natural Substrates in Cell-Free Extracts. Although caspase-3 and caspase-7 displayed almost identical activity toward the synthetic substrate DEVD-AFC, the sequence divergence between these proteins makes it likely that their interaction with natural protein substrates is nonidentical. Because residues outside of the enzyme catalytic pocket can influence acceptance of a substrate, we explored whether caspase-3 and caspase-7 also cleaved natural substrates with equal efficiency. To address this question, we added equimolar amounts of both caspases to cell-free extracts derived from Jurkat cells and assessed their ability to cleave a panel of well established caspase substrates (1). These experiments revealed that some substrates were indeed cleaved with a similar efficiency by both proteases (Fig. 2 *A* and *B*) whereas others were not (Fig. 2 *C* and *D*).

Of particular note, whereas caspase-3 and caspase-7 both cleaved proteins such as RhoGDI, PARP, ROCK I, and ICAD equally well (Fig. 2 *A* and *B*), these proteases exhibited clear differences in their activity toward XIAP and gelsolin and more modest differences toward other substrates such as Bid (Fig. 2 *C* and *D*). Whereas the majority of substrates examined were more efficiently cleaved by caspase-3 than caspase-7, cochaperone p23 was a much better substrate for caspase-7 than caspase-3 (Fig. 2 *C* and *D*). Thus, in sharp contrast to what we observed using the synthetic caspase-3/caspase-7 substrate, DEVD-AFC, the enzymatic activities of caspase-3 and caspase-7 clearly differ toward natural substrates such as gelsolin and cochaperone p23, with more modest differences seen with XIAP and Bid.

Caspase-9 Is Efficiently Processed by Caspase-3 but Not Caspase-7. In the Apaf-1/caspase-9 apoptosome-initiated caspase activation cascade, caspase-3 has been shown to mediate feedback processing on caspase-9 (4, 12). Therefore, we also explored whether caspase-7 could process caspase-9 in a similar fashion. Using *in vitro* transcribed and translated caspases, we observed that caspase-3 processed caspase-9 and caspase-6 much more efficiently than did caspase-7, based on the disappearance of the pro-forms of these proteases and the appearance of their processed forms (Fig. 2*E*). Similar results were also observed when cell-free extracts were used as a source of caspase-9 and caspase-6 (Fig. 2 *F* and *G*). Moreover, the latter experiments also demonstrated that recombinant caspase-3 also processed caspase-2 much more efficiently than recombinant caspase-7 (Fig. 2 *F* and *G*). These data suggest that caspase-3 is a more efficient enzyme than caspase-7 in terms of its ability to propagate the caspase activation cascade.

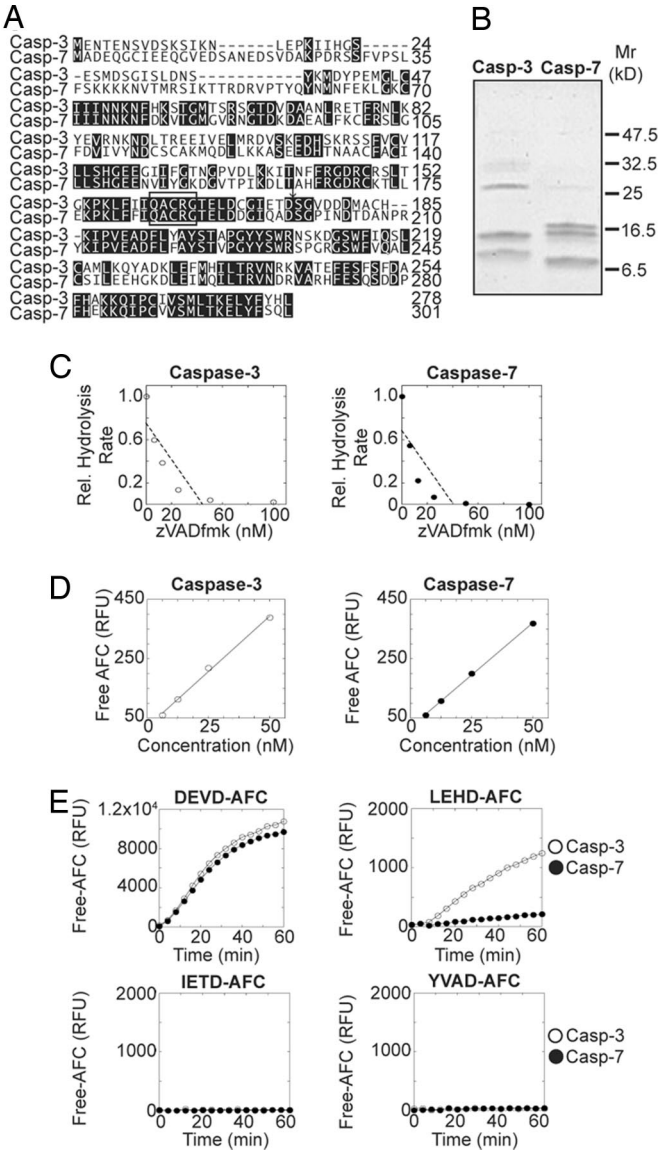

Fig. 1. Hydrolysis of synthetic substrates by human caspase-3 and caspase-7. (*A*) Sequence alignment of human caspase-3 and caspase-7. Identical residues are highlighted in black. The conserved active site residues are boxed. (*B*) SDS/PAGE analysis of purified recombinant human caspase-3 and caspase-7 visualized by Coomassie staining. Five micrograms of bacterial-derived purified proteins were loaded in each lane. (*C*) Active-site titration of recombinant human caspase-3 and caspase-7 against DEVD-AFC. Caspases were incubated at 37°C for 30 min with the indicated amounts of the irreversible caspase inhibitor zVAD-fmk followed by measurement of residual caspase activity for each treatment by fluorimetry using Ac-DEVD-AFC as a substrate. (*D*) Linear rate of hydrolysis by equimolar amounts of active caspase-3 and caspase-7 was determined by fluorimetric assay using Ac-DEVD-AFC as a substrate. (*E*) Equimolar amounts (25 nM) of recombinant caspase-3 and caspase-7 were compared for their ability to hydrolyze the indicated synthetic peptide substrates. Results are representative of three independent experiments.

Caspase-3 and Caspase-7 Display Divergent Activity Toward Purified Substrates. It was possible that some of the differences observed in the preceding experiments could be attributable to indirect effects as a result of differential activation of endogenous caspases (or other proteases) within the cell-free extracts. To

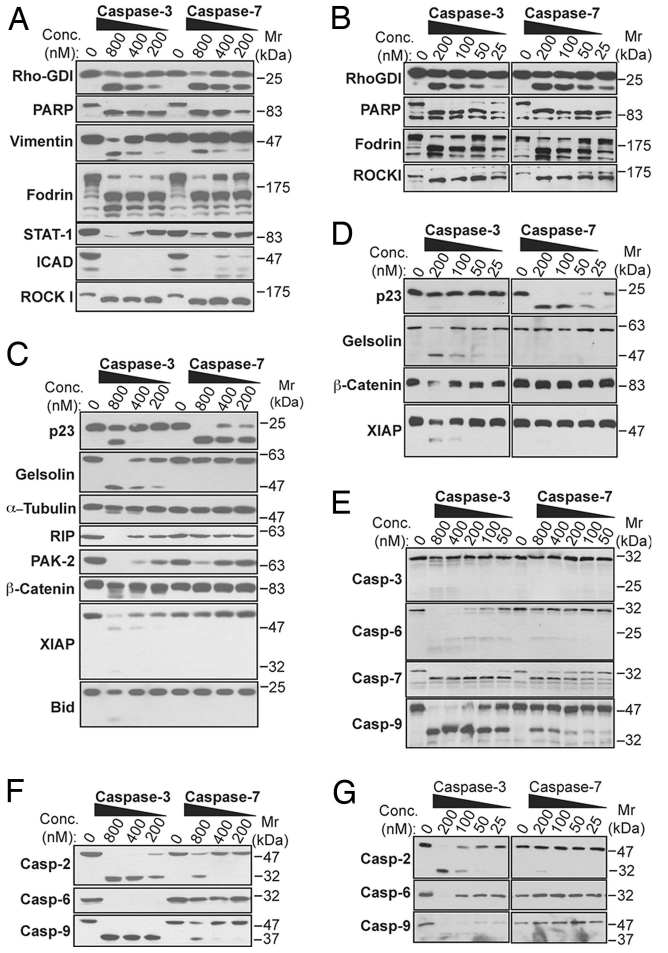

Fig. 2. Proteolysis of natural substrates and caspases by recombinant caspase-3 and caspase-7. Jurkat cell-free extracts were incubated for 2 h at 37°C with the indicated concentrations of recombinant human caspase-3 and caspase-7 followed by immunoblotting for the indicated proteins. (*A* and *B*) Substrates that were cleaved with similar efficiency by both enzymes. (*C* and *D*) Substrates exhibiting differential proteolysis by caspase-3 and caspase-7. (*E*) Proteolysis of the indicated ^{35}S-labeled caspases, prepared by *in vitro* transcription/translation, by recombinant caspase-3 and caspase-7. Reactions were carried out for 2 h at 37°C followed by SDS/PAGE and fluorography analysis. (*F* and *G*) Proteolysis of endogenous caspases by recombinant caspase-3 and caspase-7. Jurkat cell-free extracts were incubated for 2 h at 37°C with the indicated concentrations of recombinant caspase-3 and caspase-7 followed by immunoblotting for the indicated caspases. Results are representative of three independent experiments.

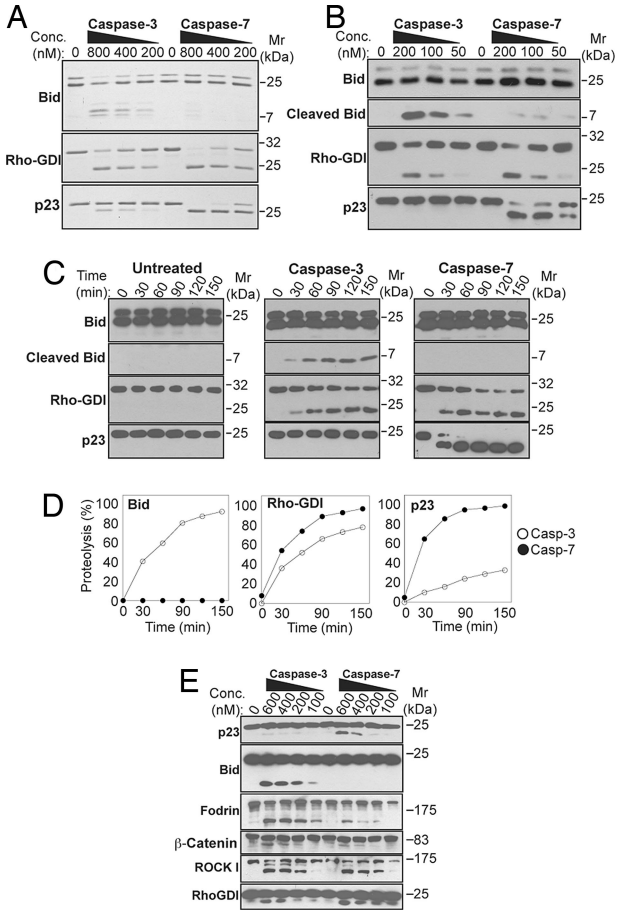

Fig. 3. Bid and cochaperone p23 exhibit differential proteolysis by human and mouse caspase-3 and caspase-7. (*A* and *B*) Recombinant Bid, Rho-GDI, and cochaperone p23 were coincubated for 2 h at 37°C with the indicated concentrations of caspase-3 and caspase-7, and reaction products were separated by SDS/PAGE and visualized by Coomassie staining (*A*) or immunoblotting (*B*). Note that recombinant Bid purified from bacteria as a doublet and both species were confirmed as Bid protein by mass spectrometry analysis. The reason for the difference in mobility of the two forms of Bid is not clear but may relate to partial misfolding of the protein. (*C*) Time-course analysis of purified Bid, Rho-GDI, and cochaperone p23 proteolysis by caspase-3 and caspase-7. Substrates were incubated at 37°C with 200 nM recombinant caspase-3 or caspase-7, and samples were taken at the indicated times. Reaction products were analyzed by SDS/PAGE and visualized by immunoblotting. (*D*) Densitometry analysis was performed to calculate the percentage of proteolysis over time for each of the treatments shown in Fig. S1 where 800 nM of each caspase was used to cleave recombinant purified Bid, Rho-GDI, or cochaperone p23. (*E*) Mouse J774 cell-free extracts were incubated for 2 h at 37°C with the indicated concentrations of recombinant mouse caspase-3 and caspase-7 followed by immunoblotting for the indicated proteins. Results are representative of three independent experiments.

exclude this possibility, we prepared recombinant purified Bid, Rho-GDI, and cochaperone p23 and assessed the efficiency of proteolysis of these substrates by caspase-3 and caspase-7 under these more stringent conditions. As Fig. 3 *A* and *B* illustrates, these experiments recapitulated what was observed in the cell-free context as Bid underwent efficient proteolysis by caspase-3 but was not cleaved by caspase-7 under the same conditions. However, the reverse was true with cochaperone p23, which was cleaved much more efficiently by caspase-7 than caspase-3 (Fig. 3 *A* and *B*). Moreover, RhoGDI was cleaved equally well by both caspases (Fig. 3 *A* and *B*). Time-course analyses further underscored the clear preferences displayed by caspase-3 and caspase-7 toward particular substrates [Fig. 3 *C* and *D* and supporting information (SI) Fig. S1]. Of note, these data also faithfully reproduced our earlier observations made in the cell-free extracts (Fig. 2 *A–D*).

To ask whether mouse caspase-3 and caspase-7 also exhibited differential activity toward natural substrates, we used mouse J774 cell-free extracts and titrated recombinant murine caspase-3 and caspase-7 into these extracts followed by immunoblotting for p23, Bid, ROCK I, and several additional substrates. As shown in Fig. 3*E*, we again observed differential proteolysis of p23 and Bid by caspase-3 and caspase-7, whereas ROCK I and RhoGDI were cleaved with a similar efficiency by the same proteases.

Immunodepletion of Caspase-3 Abolishes the Majority of Proteolytic Events Observed by Proteomic Analysis. Using Jurkat cell-free extracts immunodepleted of caspase-3, we have previously shown that this protease is absolutely required for proteolysis of

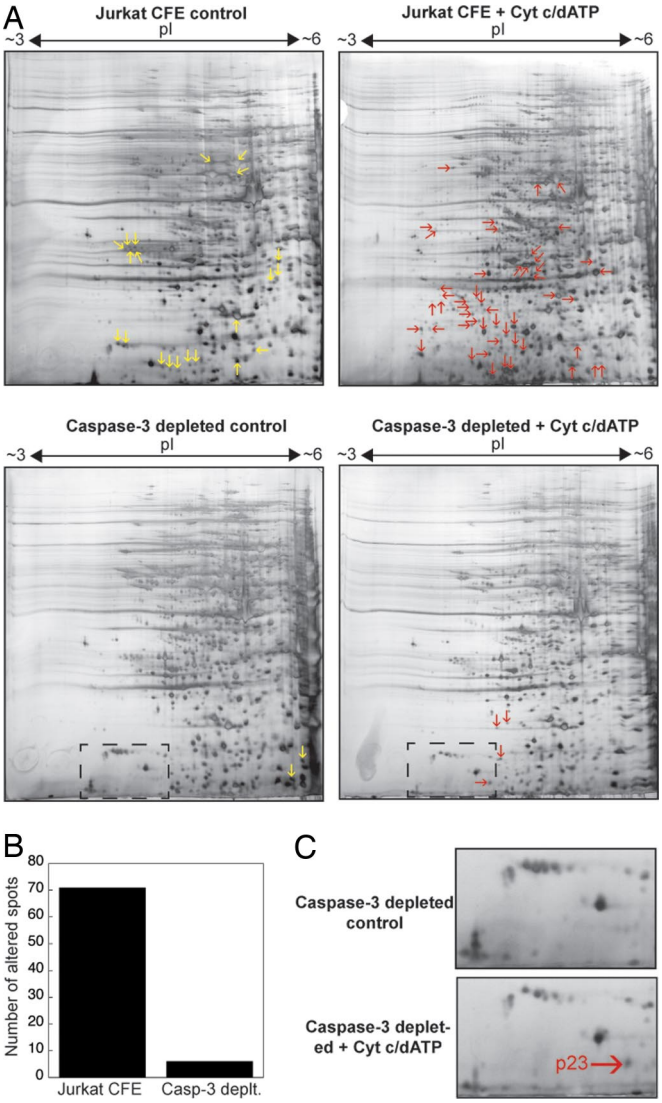

Fig. 4. Depletion of caspase-3 abrogates the majority of cytochrome *c*/dATP-induced caspase-dependent alterations to the proteome. (*A*) Mock-depleted or caspase-3-depleted Jurkat cell-free extracts were incubated for 2 h at 37°C in the presence or absence of cytochrome *c*/dATP as shown. Samples (350 μg per treatment) of each reaction were subjected to two-dimensional SDS/PAGE analysis, and proteins were subsequently visualized by silver staining. Protein spots corresponding to novel proteolytic fragments not detected on the untreated control gel are indicated by red arrows, and protein spots present in the control but not detected in cytochrome *c*/dATP-treated samples are indicated by yellow arrows. (*B*) Histogram indicating the approximate total number of alterations detected in cytochrome *c*/dATP-treated mock-depleted extracts or caspase-3-depleted extracts. (*C*) Zoomed area of the gels outlined in *A* where the protein indicated by an arrow was identified by mass spectrometry analysis as a cleaved fragment of cochaperone p23.

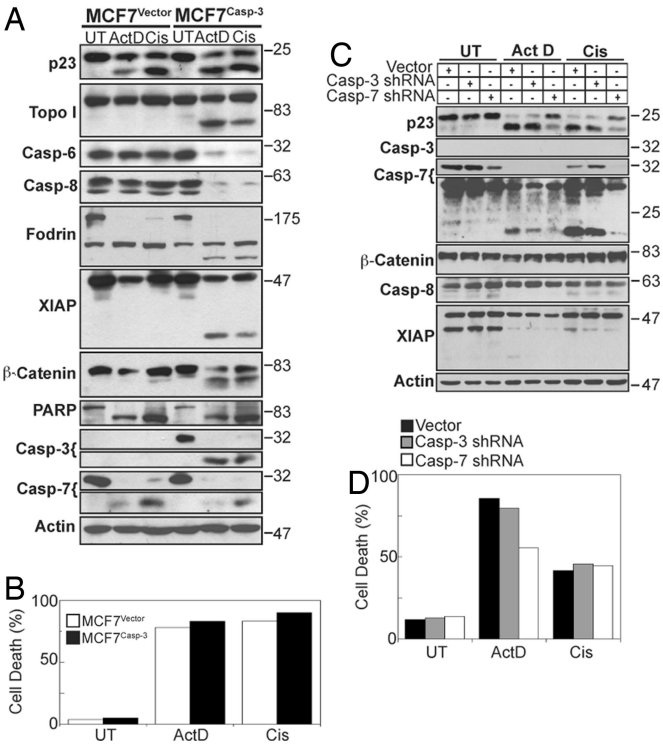

Fig. 5. *CASP-3*-deficient MCF-7 cells fail to cleave multiple caspase substrates with the exception of cochaperone p23 and PARP. (*A*) Immunoblot analysis of the indicated caspase substrates within lysates generated from caspase-3-deficent (MCF7^{vector}) or caspase-3-reconstituted (MCF7^{Casp-3}) cells that were left untreated (UT) or were cultured for 22 h in the presence of actinomycin D (ActD; 5 μM) or cisplatin (Cis; 100 μM). (*B*) Cell death counts for corresponding treatments in *A* were performed based on morphological criteria as described in *Materials and Methods*. (*C*) Immunoblots of lysates generated from caspase-3-deficient (MCF7^{vector}) cells transfected with 1 μg of either *CASP-3* or *CASP-7* shRNA plasmids for 72 h followed by treatment with ActD or cisplatin for 15 h. (*D*) Corresponding cell death counts for the cells treated in *C*. Results are representative of three independent experiments.

a small panel of caspase substrates that are typically cleaved during the terminal phase of apoptosis (11). Because the preceding experiments suggested that caspase-3 is generally more promiscuous toward the substrates examined than caspase-7 (Fig. 2), we repeated our analysis of caspase-3-depleted Jurkat extracts using two-dimensional gel analysis to enable us to visualize the impact of caspase-3 removal on a more global scale (Fig. 4). In this context, caspase activation was achieved by addition of cytochrome *c* and dATP to the extracts because these factors initiate the Apaf-1/caspase-9-dependent caspase activation cascade, which activates caspase-3 and caspase-7 downstream of caspase-9 (4). These experiments clearly demonstrated that the removal of caspase-3 abolished the vast majority of caspase-dependent proteolytic changes evident in this system, with few proteins undergoing proteolysis in caspase-3-depeleted extract (Fig. 4*B*). Interestingly, of the few proteins that did undergo proteolysis when caspase-3 was removed from the extracts, one of these was identified as co-chaperone p23 (Fig. 4*C*), confirming that this protein is one of the few preferred substrates of caspase-7.

***CASP-3*-Deficient MCF-7 Cells Are Defective in Proteolysis of Multiple Caspase Substrates.** To ask whether caspase-3 is responsible for the majority of apoptosis-associated proteolysis taking place in a cellular context, we used MCF-7^{vector} cells that are deficient in the expression of caspase-3 because of a spontaneous deletion within the CASP-3 gene (13). As Fig. 5*A* illustrates, proteolysis of a range of caspase substrates was greatly impaired in caspase-3-deficient MCF-7 cells, as compared with caspase-3-reconstituted MCF-7 cells (MCF-7^{Casp-3}), despite both cell lines dying with similar kinetics in response to the same treatments (Fig. 5*B* and Fig. S2). However, proteolysis of cochaperone p23 and PARP, both of which were found to be excellent substrates for caspase-7 (Fig. 2 *A–D*), was unaffected by the absence of caspase-3 (Fig. 5*A*). Furthermore, shRNA-mediated knockdown of caspase-7 substantially inhibited cochaperone p23 proteolysis under the same conditions, arguing that caspase-7 is indeed

responsible for the proteolysis of this protein during the demolition phase of apoptosis (Fig. 5 *C* and *D*).

Collectively, these results provide a biochemical basis for the distinct phenotypes observed in cells and mice lacking caspase-3 or caspase-7. Caspase-3 appears to be a more promiscuous protease, a result that correlates with what is generally a more severe set of defects linked with *CASP-3* deficiency. However, a degree of redundancy does appear to exist between these two enzymes toward certain substrates, such as PARP, Fodrin, and ROCK I. Of the 20 different substrates examined during this study, 12 were preferentially cleaved by caspase-3 whereas only one (cochaperone p23) was more susceptible to proteolytic processing by caspase-7. If this picture is representative it suggests that, although these enzymes are closely related and both are activated during the demolition phase of apoptosis (14), caspase-3 and caspase-7 are clearly distinct proteases and occupy nonredundant roles within the cell death machinery.

Materials and Methods

Materials. The following antibodies were used: anti-Rho-GDI/D4-GDI, anti-PARP, anti-STAT1, anti-ROCK-1, anti-gelsolin, anti-RIP, anti-catenin, anti-XIAP, and anti- BID (BD Biosciences); anti-α-tubulin (ICN); anti-p23 (Affinity Bioreagents); anti-DFF45/ICAD (Upstate); anti-Fodrin (Chemicom); anti-Vimentin (Sigma); and anti-PAK2 (Cell Signaling). The peptides zVAD-fmk, Ac-DEVD-AFC, Ac-LEHD-AFC, Ac-IETD-AFC, and Ac-YVAD-AFC were purchased from Bachem. Unless otherwise indicated, all other reagents were purchased from Sigma.

Expression and Purification of Recombinant Proteins. The pET23b expression plasmids containing full-length human caspase-3 and caspase-7 were kindly provided by Guy Salvesen (Burnham Institute, La Jolla, CA). Murine *CASP-3* and *CASP-7* were cloned into pET45b. The pET15b expression plasmid, encoding full-length human Bid, was kindly provided by Xiao-Ming Yin (University of Pittsburgh School of Medicine, Pittsburgh, PA). Full-length cochaperone p23 was expressed from a pET45b expression plasmid. For protein expression, plasmids were transformed into the bacterial *Escherichia coli* strain BL21 (DE3) and were expressed and affinity-purified as previously described (15).

Cell-Free Reactions. Cell-free cytosolic S-15 extracts were generated from human Jurkat and mouse J774 cells as previously described (4, 16). Typically, extracts were normalized to 10 mg/ml total protein content and were then diluted 2-fold in cell-free extract buffer (20 mM Hepes, pH 7.5/10 mM KCl/1.5 mM $MgCl_2$/1 mM EDTA/1 mM EGTA/1 mM DTT/100 μM PMSF/10 μg/ml leupeptin/2 μg/ml aprotinin). Recombinant caspase-3 and caspase-7 were added to the reactions at final concentrations indicated in the figure legends. Reactions were incubated for 2 h at 37°C to facilitate caspase-mediated proteolysis.

Caspase Activity Assays. Reactions (100-μl final volume) were carried out in protease reaction buffer (50 mM Hepes, pH 7.4/75 mM NaCl/0.1% CHAPS/2 mM DTT) containing 50 μM Ac-DEVD-AFC, Ac-LEHD-AFC, Ac-IETD-AFC, or Ac-YVAD-AFC. Samples were measured by using an automated fluorimeter (Spectrafluor Plus; TECAN) at wavelengths of 430 nm (excitation) and 535 nm (emission).

Active Site Titration of Caspases. Recombinant human or murine caspase-3 and caspase-7 were incubated with a range of concentrations (0, 6.25, 12.5, 25, 50, and 100 nM) of zVAD-fmk for 30 min at 37°C. Residual caspase activity was then determined by monitoring the hydrolysis of Ac-DEVD-AFC as described above.

Image Acquisition and Analysis. Western blot images were scanned from x-ray film and uniformly adjusted for brightness and contrast by using Photoshop software (Adobe Systems). Coomassie blue-stained gels were captured by digital camera (CoolPix 5000; Nikon), and uniform adjustments were again performed in Photoshop. Densitometric analysis of gels was preformed by using ImageJ software.

Two-Dimensional Gel Analysis. Two-dimensional SDS/PAGE analysis was performed by using either mock-depleted or caspase-3-depleted Jurkat cell-free extracts, as previously described (17). Briefly, 350 μg of protein from each reaction was subjected to isoelectric focusing in the first dimension on pH 3–6 immobilized pH gradient strips (Bio-Rad) followed by 12% SDS/PAGE in the second dimension. Proteins were subsequently visualized by silver staining as previously described (15, 17).

Assessment of Apoptosis. Apoptosis was assessed by using standard morphological criteria such as cellular retraction, membrane blebbing, and cellular detachment from the plate (14).

ACKNOWLEDGMENTS. We thank Dr. Guy Salvesen for providing expression plasmids for human caspase-3 and caspase-7, Dr. Alan G. Porter for providing MCF-7^{vector} and MCF-$7^{Casp\text{-}3}$ cell lines, and Dr. Jin Wang for providing caspase-3 and caspase-7 shRNA plasmids. S.J.M. is a Science Foundation Ireland Fellow (PI1/B038). We thank Science Foundation Ireland for their support of this work. J.G.W. and C.S. are the recipients of postgraduate studentship awards from the Irish Research Council for Science, Engineering and Technology.

1. Lüthi AU, Martin SJ (2007) The CASBAH: A searchable database of caspase substrates. *Cell Death Differ* 14:641–650.
2. Timmer JC, Salvesen GS (2007) Caspase substrates. *Cell Death Differ* 14:66–72.
3. Stennicke HR, *et al.* (1998) Pro-caspase-3 is a major physiologic target of caspase-8. *J Biol Chem* 273:27084–27090.
4. Slee EA, *et al.* (1999) Ordering the cytochrome c-initiated caspase cascade: Hierarchical activation of caspases-2, -3, -6, -7, -8, and -10 in a caspase-9-dependent manner. *J Cell Biol* 144:281–292.
5. Thornberry NA, *et al.* (1997) A combinatorial approach defines specificities of members of the caspase family and granzyme B: Functional relationships established for key mediators of apoptosis. *J Biol Chem* 272:17907–17911.
6. Stennicke HR, Renatus M, Meldal M, Salvesen GS (2000) Internally quenched fluorescent peptide substrates disclose the subsite preferences of human caspases 1, 3, 6, 7 and 8. *Biochem J* 350:563–568.
7. Kuida K, *et al.* (1996) Decreased apoptosis in the brain and premature lethality in CPP32-deficient mice. *Nature* 384:368–372.
8. Houde C, *et al.* (2004) Caspase-7 expanded function and intrinsic expression level underlies strain-specific brain phenotype of caspase-3-null mice. *J Neurosci* 24:9977–9984.
9. Lakhani SA, *et al.* (2006) Caspases 3 and 7: Key mediators of mitochondrial events of apoptosis. *Science* 311:847–851.
10. Leonard JR, Klocke BJ, D'Sa C, Flavell RA, Roth KA, (2002) Strain-dependent neurodevelopmental abnormalities in caspase-3-deficient mice. *J. Neuropathol. Exp Neurol* 61:673–677.
11. Slee EA, Adrian C, Martin SJ (2001) Executioner caspase-3, -6, and -7 perform distinct, non-redundant roles during the demolition phase of apoptosis. *J Biol Chem* 276:7320–7326.
12. Srinivasula SM, Ahmad M, Fernandes-Alnemri T, Alnemri ES (1998) Autoactivation of procaspase-9 by Apaf-1-mediated oligomerization. *Mol Cell* 1:949–957.
13. Jänicke RU, Sprengart ML, Wati MR, Porter AG (1998) Caspase-3 is required for DNA fragmentation and morphological changes associated with apoptosis. *J Biol Chem* 273:9357–9360.
14. Taylor RC, Cullen SP, Martin SJ (2008) Apoptosis: Controlled demolition at the cellular level. *Nat Rev Mol Cell Biol* 9:231–241.
15. Hill MM, Adrian C, Duriez PJ, Creagh EM, Martin SJ (2004) Analysis of the composition, assembly kinetics and activity of native Apaf-1 apoptosomes. *EMBO J* 23:2134–2145.
16. Martin SJ, *et al.* (1996) The cytotoxic cell protease granzyme B initiates apoptosis in a cell-free system by proteolytic processing and activation of the ICE/CED-3 family protease, CPP32, via a novel two-step mechanism. *EMBO J* 15:2407–2416.
17. Adrain C, Murphy BM, Martin SJ (2005) Molecular ordering of the caspase activation cascade initiated by the cytotoxic T lymphocyte/natural killer (CTL/NK) protease granzyme B. *J Biol Chem* 280:4663–4673.